

# Mid-IR Observations of T Tauri stars: Probing the Star-Disk Connection in Rotational Evolution

Praveen Kundurthy and Michael R. Meyer

*Steward Observatory, The University of Arizona, Tucson, AZ 85721*

pkundurthy@as.arizona.edu, mmeyer@as.arizona.edu

Massimo Robberto and Steven V.W. Beckwith

*Space Telescope Science Institute, Baltimore, MD 21218*

robberto@stsci.edu, svwb@stsci.edu

Tom Herbst

*Max-Planck-Institut für Astronomie, Heidelberg D-69117, Germany*

herbst@mpia-hd.mpg.de

## ABSTRACT

We present mid-IR N-band ( $\lambda_{eff} = 10.2\mu\text{m}$ ) photometry of a carefully selected sample of T Tauri stars thought to be single from the Taurus-Auriga molecular cloud. Infrared excesses in these stars are generally attributed to circumstellar dust-disks. Combining observations at  $2.16\mu\text{m}$  ( $K_s$ -band) and  $10.2\mu\text{m}$  (N-band) we probe a region in the circumstellar dust-disk from a few stellar radii through the terrestrial planet zone (0.02-1.0AU). By analyzing the distribution of the  $(K_s - N)$  color index with respect to previously measured photometric rotation periods we investigate what role circumstellar disks play in the rotational evolution of the central star. The resulting positive correlation between these two variables is consistent with the notion that a star-disk interaction facilitates the regulation of angular momentum during the T Tauri stage. We also demonstrate, how including non-single stars in such an analysis will *weaken* any correlation in the relation between  $(K_s - N)$  color and period. To further understand disk properties we also present SEDs for a few objects with new ground based M-band ( $\lambda_{eff} = 4.8\mu\text{m}$ ) and Q-band ( $\lambda_{eff} = 20\mu\text{m}$ ) data and compare them to a geometrically thin, optically-thick disk model.

*Subject headings:* stars:pre-main sequence – stars:rotation – infrared: photometry – ISM:individual(Taurus,Auriga) – circumstellar matter: disks

## 1. Introduction

As a rotating molecular cloud core collapses to form a star it must shed vast amounts of angular momentum to explain the observed differences between the specific angular momentum of molecular cloud cores and stars on the main-sequence (Bodenheimer 1995). Various physical processes, which serve as solutions to this “angular momentum problem” are thought to occur as an object transitions from a cloud core to a Zero-Age Main Sequence (ZAMS) star. For low-mass stars in the pre-main sequence stage (T Tauri stars) the regulation of stellar rotational angular momentum is thought to be facilitated by the formation of and subsequent interaction with a circumstellar disk. Circumstellar disks are thought to be common by-products of the star formation process (Beckwith & Sargent 1996). They are easily identified by peculiar features like infrared and ultraviolet excesses, and in some rare circumstances can also be detected through direct imaging (O’Dell 1993; McCaughrean & O’Dell 1996). Kenyon & Hartmann (1995) estimate  $> 50\%$  of stars in the Taurus-Auriga star forming region have circumstellar disks, while Hillenbrand et al. (1998) estimate that  $> 80\%$  of stars in the Trapezium cluster possess circumstellar accretion disks (see also Haisch, Lada & Lada 2001). The IR excesses from these disks are the result of heating circumstellar gas and dust by radiation from the central star and through viscous accretion. The disk temperature distribution is often modeled as a power-law. If the disk is optically thick it will radiate as a blackbody with the shortest wavelengths dominated by higher temperature material in the inner disk and the longer wavelengths dominated by cooler material in the outer regions (Beckwith 1999). Thus, emission at different wavelengths can be used to probe different regions in the disk.

The pioneering study by Edwards et al. (1993) for a set of stars from the Taurus, Auriga, Chameleon, Orion and Lupus star-forming regions, compared stellar rotation periods with the  $(H - K)$  color index. This color index probes a region in the disk that lies within a few stellar radii ( $\sim 10R_{\odot}$ ). They found stars whose  $(H - K)$  colors indicated the presence of an accretion disk were rotating more slowly than stars whose  $(H - K)$  colors indicated the absence of an accretion disk. A similar study by Bouvier et al. (1993) suggested a bimodal distribution of slowly rotating classical T Tauri stars (cTTS, showing evidence of active accretion from a circumstellar disk) and fast rotating weak T Tauri stars (wTTS, weak-lined  $H\alpha$  emission-line stars with no signs of accretion). Studies of the Orion Nebula Cluster (ONC) have yielded mixed results. Choi & Herbst (1996) report a bimodal distribution in photometric periods of T Tauri stars in Orion as evidence for the disk-locking phenomena (see also Herbst et al. 2002). Theoretical models have always relied heavily on some form of direct or indirect angular momentum transfer between stars and their disks to explain the redistribution of rotational angular momentum during the transition from the Pre-Main Sequence (PMS) stage to the ZAMS stage. However, an extensive study conducted by

Stassun et al. (1999, 2001) report no bi-modality in period distribution and no dichotomy of disked slow rotators and disk-less fast rotators. A recent review of this literature can be found in Mathieu (2004). In this study we use the  $(K_s - N)$  color index to probe a region in T Tauri dust-disks that extends from a few stellar radii through the terrestrial planet zone (0.02-1.0AU). Comparing the  $(K_s - N)$  color index of carefully selected single stars with previously measured rotation periods allows us to investigate any effects the disk might have on the angular momentum of the star.

This paper outlines an observational study that expands on the work presented in Meyer & Beckwith (1997), and hopes to further our understanding of the role of disks in the rotational evolution of T Tauri stars. In section 2 we present a description of our sample, the observations and the data reduction procedure. In section 3 we present the relationship between the  $(K_s - N)$  color index and rotation period of single PMS stars in Taurus-Auriga, and the spectral energy distributions (SEDs) of a few stars with new M and Q-band data. In section 4 we discuss the results in light of current theories for the rotational evolution of T Tauri star and disk systems. We also demonstrate that including binaries in a study of  $(K_s - N)$  vs. rotation period diminishes any observed correlation. We conclude with a summary in section 5.

## 2. Observations and Data

We selected stars in the Taurus-Auriga SFR, that have been surveyed for, but are known to be lacking companions from the multiplicity surveys of Ghez et al. (1993), Leinert et al. (1993) and Simon et al. (1995), that also have photometric period data available in the literature. Photometric period data for all stars were taken from Bouvier et al. (1993, 1995) and Osterloh et al. (1996). Infrared  $K_s$ -band data for all stars were taken from the Two-micron all sky survey (2MASS), point-source catalog. The typical magnitude uncertainties for the  $K_s$ -band data ranged between 2% – 3% for the stars of our sample. We obtained new N-band observations for 12 stars. The details of the observations, such as filter information, exposure times, and flux standards are listed in Table 1. We selected 18 more stars that satisfied the selection criterion above and also had N-band measurements in the literature with photometric uncertainties  $\leq 30\%$ . The N-band magnitudes were queried in the catalog Gezari et al. (1999) and references therein. The original literature source of N-band magnitudes are noted in the last column of Table 2. When multiple measurements of an object were returned from Gezari et al. (1999) we chose the most recent measurement or the measurement with the smallest magnitude uncertainty. Table 2 also lists spectral types, T Tauri types, SED classes, photometric periods, effective temperatures and luminosities for

all 30 objects in our sample (Bouvier et al. 1993, 1995; Osterloh et al. 1996; Strom et al. 1989; Kenyon & Hartmann 1995). The sample covers an age range of 0.1 - 10Myrs, and a mass range of  $0.2 - 2.0M_{\odot}$ . The ages and masses were estimated from the tracks of D’Antona & Mazzitelli (1997) and typically have uncertainties of order  $\times 2$ . The ratio of CTTS to WTTS in our sample is 14:15. The vast majority of objects in our sample are optically visible Pre-Main Sequence stars with class II or class III SEDs and well-determined spectral types. However, we do include a heavily veiled object FT Tau, a continuum star of SED class II.

We also made N-band observations of the binary star UX Tau (see Table 1). M and Q-band observations (see Table 1) for a few single stars were also made in order to derive SEDs that might illuminate properties of circumstellar disks surrounding these individual sources.

## 2.1. Observations

M, N and Q-band photometric observations were made using the Mid-infrared Array eXpandable (MAX; Robberto & Herbst (1998)) camera at the 3.8m United Kingdom Infrared Telescope (UKIRT) on the nights of February 6th and 8th, 1997. The MAX camera was built by Infrared Laboratories of Tucson and contains a  $128 \times 128$  pixel Rockwell HF16 Si:As BIB detector. The plate-scale of the detector was  $0.265''/\text{pixel}$  and corresponded to a field size of  $33.9'' \times 33.9''$  on UKIRT. The typical observing mode of chopping and beam switching were utilized to take images of standard stars and program stars with matched chopping and beam-switching amplitudes of approximately  $10.3''$ . Spatial and temporal variations of the sky emission in the mid-IR were reduced by this observational procedure. Typical integration times ranged from 10.24-20.48 seconds for all bands. These chop-subtracted frames were co-added and the resulting total integration times are listed in Table 1. The typical read noise and gain values for this detector were 1250 e- and 400 e-/ADU respectively.

## 2.2. Data Reduction

Each chop-subtracted frame contained two signals, one negative and one positive, of the source placed approximately  $10.3''$  apart. The frames were cleaned for cosmic rays using a 3-sigma rejection procedure and then combined through subtraction of beam-switched pairs of similar frames of the same object to create a final image with one central positive signal and two satellite negative signals. Additional bad pixels were identified by eye and

interpolated over using adjacent pixels with FIXPIX in IRAF<sup>1</sup>. The PHOT task in IRAF’s NOAO.DIGIPHOT.APPHOT package was used to derive aperture photometry on the central signals in each object frame. The optimal aperture was selected such that the combined uncertainties due to PSF fluctuations (resulting in uncertainties in aperture corrections) and uncertainties in the sky from larger apertures were minimized. The standard stars listed in the last column of Table 1 were used to determine the optimal apertures for each band. For the N-band, a target aperture of  $R = 2.65''$  (10 pixels) was used. A sky-annulus to determine the mean residual background was chosen such that significant source flux was excluded and the error in mean sky (within the annulus) was minimized. For the N-band the sky annulus used extended from  $5.035''$ - $5.698''$  (19 - 21.5 pixels). Photometric precision ranged from 3% – 9% for most targets in the N-band except for HD 283572 and LkCa 21 with 18% and 25% photometry respectively. Magnitude upperlimits were derived for non-detections TAP 26, TAP 40, TAP 41 and V830 Tau. We assumed a minimum object area of 4 pixels( $2 \times 2$ ) to estimate a  $3\sigma$  flux upper-limit in each respective non-detection frame. These upper limits correspond to unusually large source fluxes due to the high sky-noise in the non-detection frames. Similar photometric techniques were used for the M-band and Q-band data. The M-band target aperture was  $R = 2.915''$  (11 pixels) with a sky annulus from  $5.035'' - 5.963''$  (19 - 22.5 pixels). The Q-band target aperture was  $R = 1.855''$  (7 pixels) with a sky annulus from  $2.915'' - 7.155''$  (11 - 27 pixels). For comparison, the diffraction limited diameters of the 3.8m UKIRT beam at wavelengths of interest are  $0.33''$ ,  $0.66''$  and  $1.3''$  at  $4.8\mu\text{m}$ ,  $10.2\mu\text{m}$  and  $20\mu\text{m}$  respectively. Zero-point fluxes for the standard stars in the filters used were taken from Cohen et al. (1992). The N-band photometry is presented in Tables 2 and 4 for 12 single T Tauri stars and one binary, UX Tau A. M-band photometry for two stars, and Q-band photometry for five stars is presented in Table 3.

### 3. Results

To investigate whether there is a trend of disked slow rotators and disk-less fast rotators among T Tauri stars, we plot the  $(K_s - N)$  color index against the photometric rotation period of single T Tauri stars from the Tau-Aur molecular cloud in Figure 1a. We tested for a correlation between  $(K_s - N)$  and period using a linear least-squares analysis on the data of Figure 1a. A first order polynomial was fit to the data. The fit resulted in a correlation coefficient of 0.52 for 25 data points (excluding 5 non-detections). This indicates

---

<sup>1</sup>IRAF is distributed by the National Optical Astronomy Observatories, which are operated by the Association of Universities for Research in Astronomy, Inc., under cooperative agreement with the National Science Foundation.

that the probability the variables in this linear fit are uncorrelated is  $< 0.009$ . In order to remove scatter in the correlation, we repeated this analysis explicitly taking into account the intrinsic colors and extinction of each source. We adopted the infrared extinction law from Cohen et al. (1982) and used visual reddening values ( $A_v$ ) reported by Kenyon & Hartmann (1995) for our sample of objects. We estimated intrinsic  $(K_s - N)_o$  values from Mamajek et al. (2004). Figure 1b shows the quantity  $E(K_s - N)_o$  plotted against the rotation period. Where  $E(K_s - N)_o = (K_s - N) - 0.06A_v - (K_s - N)_o$ , is the difference between reddening corrected color observed and intrinsic color (cf. Meyer et al. (1997a)). A linear least-squares analysis results in a correlation coefficient of 0.48 for 25 data points. The probability that these variables are uncorrelated is  $< 0.016$ . This is consistent with the previously derived correlation. A positive correlation could be interpreted as evidence for disk-assisted regulation of stellar angular momentum among single T Tauri stars in Taurus-Auriga. It is important to note that the observed magnitude uncertainties were not used to weight the fit since they represent photometric uncertainties from many non-simultaneous observations in the  $K_s$  and N-bands. These are much smaller than the expected range of variability in the infrared (Rydgren 1984; Skrutskie et al. 1996) which presumably contributes to the observed scatter in the correlations. Figure 1a and 1b are marked by horizontal dashed lines that designate important limits in the distributions of the  $(K_s - N)$  and  $E(K_s - N)_o$  color indices. The line at  $(K_s - N) = 2.0m$  in Figure 1a represents the expected lower limit for an excess from a face-on, optically-thick and geometrically-thin disk (Hillenbrand et al. 1992). Taking into account the extinction, for the objects in our sample, the same limit falls at  $E(K_s - N)_o = 1.8m$  in Figure 1b. The dashed line in Figure 1a at  $(K_s - N) = 1.0m$  marks the expected maximum color for a normal reddened photosphere, and the line in Figure 1b at  $E(K_s - N)_o = 0.84m$  marks the value of a 3-sigma excess from the dispersion of intrinsic colors for stars in our sample (Mamajek et al. 2004). This is the lower limit for the detection of a disk.

Figure 2 shows the histogram of  $(K_s - N)$  values of the stars in our sample separated into bins of  $0.5m$ . There is a paucity of stars between  $1.0m < (K_s - N) < 2.0m$ . This confirms the findings of Skrutskie et al. (1990) (see also Simon & Prato 1995; Kenyon & Hartmann 1995; Wolk & Walter 1996) that so-called “transition objects” within this color range are rare. It suggests that the time to evolve from optically-thick to optically-thin in the 0.02-1.0 AU region is short compared to the average age of T Tauri stars (i.e.  $\ll 1$  Myr). The only star within this region is DH Tau ( $(K_s - N) = 1.92m$  and  $E(K_s - N)_o = 1.53$ ).

We classified objects from Figures 1a and 1b into disked and disk-less stars and compared their period distributions. Objects with  $(K_s - N) < 1.0m$  or  $E(K_s - N)_o < 0.84m$ , were classified as disk-less and objects with  $(K_s - N)$  and  $E(K_s - N)_o$  greater than these respective limits were classified as disked. The two sets contained the same objects for Figure 1a and

1b. We found stars with disks rotate slower on average ( $P_{avg} = 7.46d$ ) and stars without disks rotate faster ( $P_{avg} = 4.30d$ ). The period distributions are wide for both ( $\sigma = 2.44$  and  $2.57$  for disked and disk-less respectively). A two sided K-S test of the period distribution of disked and disk-less stars resulted in  $D = 0.68$ . Which indicates the probability that the period distributions are drawn from the same parent is 1.6%. In the language of gaussian hypothesis testing, this is a  $2.4\sigma$  result. So for stars which are believed to be single, the period distributions of disked and disk-less stars, are marginally different.

As described in section 2, we obtained M-band and Q-band photometry for a few stars with strong IR excesses. All new M and Q-band photometry are listed with other photometry assembled from the literature in Table 3. SEDs derived from these data are shown in Figure 3. The data are not simultaneous. We compared the de-reddened fluxes to empirical stellar photospheres appropriate for each spectral type and models of geometrically-thin, optically-thick disks (Hillenbrand et al. 1992). The model is of a face-on blackbody disk extending from the stellar surface. Easily visible in all SED plots are signs of accretion as the excess fluxes in the U-band ( $\lambda_{eff} = 0.36\mu\text{m}$ ). IR excesses are also present and significantly exceed the predictions of the stellar photosphere and the flat reprocessing disk model at longer wavelengths. Most sources lack IR excesses at the shortest wavelengths, consistent with dust sublimation and/or inner holes (Muzerolle et al. (2003); cf. Meyer et al. (1997a)). An inner dust disk hole would be visible as a lack of near-infrared excess in the SED. Disk regulation theories predict that circumstellar disks have inner holes maintained by pressure balance with the stellar magnetic field (Ostriker & Shu 1995). Measurements of stellar magnetic field strengths are needed along with estimates of  $M_*$ ,  $\dot{M}$  and  $R_*$  to properly estimate the extent of inner disk clearing. The very large IR excesses at longer wavelengths indicate that the disks are probably not flat but flared (Chiang & Goldreich 1997) with vertical temperature structures commonly referred to as “disk atmospheres” (see D’Alessio et al. 1999; Dullemond et al. 2001).

#### 4. Discussion

In the following sections we discuss the significance of our results in the context of current theoretical frameworks for rotational evolution. We also compare our observational study to others conducted in Tau-Aur and the ONC. Finally we emphasize the importance of sample selection criteria for studying rotational evolution of low mass PMS stars.

#### 4.1. Disk-regulation

The positive correlation, at the 99% confidence level, between the  $(K_s - N)$  color index and rotation period supports the idea that disks play a role in regulating the angular momentum of T Tauri stars. Most models of PMS angular momentum evolution rely on some form of disk-assisted angular momentum regulation. In the absence of a disk, we would expect young stars to conserve total angular momentum as they contract towards the ZAMS, spinning-up as their radii decrease over time. Our results suggest that the disk is countering the spin-up effect caused by ordinary stellar contraction and to some extent the spin-up torque caused by the accretion of high angular momentum material from the disk boundary (Ghosh & Lamb 1979a,b). Evidence for accretion is seen in the U-band excess (Figure 3) of even the fast rotator GK Tau. Camenzind (1990), Königl (1991) and Cameron & Campbell (1993) explore the idea of magnetospheric star-disk coupling. In this model the stellar magnetic field is thought to couple with the disk, extending to regions where the disk is spinning slower than the stellar surface. As a result the star is braked and eventually slows its rotation significantly. Shu et al. (1994) and Ostriker & Shu (1995) suggest it is unlikely for magnetic coupling to occur over extended regions of the disk. Their models allow for the disk to be penetrated by the stellar magnetic field only near the co-rotation radius, hence making the transfer of angular momentum via rotational coupling insignificant. Instead, angular momentum is lost from the stellar surface through the expulsion of X-winds (eXtraordinary winds) near the star-disk boundary. The magnetized X-winds are driven by accretion from the disk. Similarly von Rekowski & Brandenburg (2004) and Matt & Pudritz (2005) explore a scenario where angular momentum is lost via accretion-powered stellar winds. In all theoretical frameworks (disk-locking, X-winds or stellar winds) the presence of an extended disk (0.02-1.0AU) is vital to angular momentum regulation. The magnetospheric disk locking models require an extended magnetized disk beyond the co-rotation radius to provide a spin-down torque. The wind models require the presence of accretion from the inner disk, which in turn depends on the extended disk to persist.

T Tauri stars are thought to dissipate their disks over a range of times during their evolution (Strom et al. 1989; Skrutskie et al. 1990; Haisch, Lada & Lada 2001). We conducted a two-sided Kolmogorov-Smirnov(K-S) test to see if the age distributions for disked and disk-less stars (as defined by the  $(K_s - N)$  index) in our sample are similar. We derived a D-statistic of 0.32 indicating that the age distributions are consistent with having been drawn from the same parent population. If disk-assisted regulation is a dominant force the angular momentum evolution of a T Tauri star, then the fact that stars dissipate their disks at different times would explain the wide dispersion of rotational rates observed for stars on the ZAMS (Bouvier, Forestini & Allain 1997; Krishnamurthi et al. 1997). In other words stars that dissipate their disks early are believed to spin-up and become rapid rotators,



while stars that dissipate their disks late, end up as slow rotators (Bouvier 1994; Rebull et al. 2004; Herbst & Mundt 2005).

## 4.2. Sample Selection

Most rotational evolution models explore only the case of a single star’s interaction with its disk. Comparing the  $(K_s - N)$  index with the rotation period of single stars enables us to compare our results to the theoretical frameworks which use single star + disk scenarios. Furthermore, there is some evidence that the presence of a companion affects the evolution of a disk around a PMS object (Meyer et al. 1997b; Ghez et al. 1994). Jensen et al. (1996) and Jensen & Mathieu (1997) present convincing evidence that disks from 50-100AU are affected by the presence of binary companions over this range of separations.

In Figure 4 we combine data points from Figure 1 with  $(K_s - N)$  and period data available for unresolved binaries (listed in Table 4). Performing a linear correlation test similar to the one described in section 3, for  $(K_s - N)$  vs. rotation period, resulted in a correlation coefficient of 0.35, for 38 data points (not including upper-limits). This means the probability that linear correlation is random is  $< 0.05$ , suggesting that the presence of unresolved binaries in a sample of young stars could *weaken* any expected correlation. We also conducted a two sided K-S test on the objects in Figure 4, separating them into disked and disk-less stars, as described in section 3. We derived a D-statistic of 0.45, which indicates that the probability the distributions are similar is 7.0%. This is a  $1.0\sigma$  result. So we cannot confidently assert that the period distributions were drawn from different parent populations. Ghez et al. (1993) estimate that 2/3 of the stars in the Tau-Aur region are multiple systems. Yet, the linear correlation test only includes 13 binary systems compared to the 25 single systems (excluding upperlimits). This is because there is a lack of photometric period data for approx 85% of the stars surveyed to be multiple systems, compared to 50% for those surveyed to be single systems (Ghez et al. 1993; Leinert et al. 1993; Simon et al. 1995; Bouvier et al. 1993, 1995; Osterloh et al. 1996). This is probably due to the difficulty in interpreting data from binary systems. Most photometric period surveys that include binaries do not resolve companions and hence it is hard to know for certain a) which component’s period was determined (if the stars are of comparable brightness) or b) if the light fluctuations were due to orbital motions (eclipsing) or actual rotational motion (spots). In addition, components in a close binary system are hard to resolve in the infrared. The source of N-band flux from an unresolved multiple system cannot be easily determined. Contributions from each stellar component, the dust disk around each object, or a circumbinary disk (Ghez et al. 1994) could add to the N-band flux. In investigating star-disk interactions in the PMS, it is important

to restrict the sample to well-studied single stars, or resolved binaries.

### 4.3. Resolving Apparent Discrepancies

The results from Edwards et al. (1993) for the  $(H - K)$  color index shows evidence for disk-less fast rotators and disked slow rotators in Tau-Aur. However, the  $(H - K)$  color index probes a region in the dust-disk very close to the stellar surface (approx  $< 0.02$  AU). Muzerolle et al. (2003) estimate that the typical temperature at which dust sublimates around T Tauri stars is approximately 1400K, which roughly corresponds to the temperatures of the hottest dust emitting in  $K_s$  ( $\lambda_{eff} = 2.16\mu\text{m}$ ) and L-band ( $\lambda_{eff} = 3.54\mu\text{m}$ ). So emission from the dust-disk is limited to the region with  $T_{disk} < 1400K$ . If we consider a case where the disk truncation radius lies far beyond the sublimation zone (where  $T_{inner-disk} \ll 1400K$ ) at  $r_{inner} \gg 0.02AU$ , the disk might still be effectively disk-locked but will not display any excess in H and K-bands. There are 8 stars from our single star set which are also studied by Edwards et al. (1993). Interestingly, 1 of the 8 stars (DN Tau) lacks a  $(H - K)$  excess but *does display a  $(K_s - N)$  excess* ( $P_{rot} = 6.0$  days). This could mean that its disk is truncated outside of the sublimation radius. The other 7 stars either lack both  $(H - K)$  and  $(K_s - N)$  excesses or display both  $(H - K)$  and  $(K_s - N)$  excesses. There are *no cases* where an object lacks a  $(K_s - N)$  excess but shows an  $(H - K)$  excess.

In a complementary study, Stassun et al. (1999) surveyed a large sample of stars in the ONC at near-IR wavelengths, with periods  $< 8.0$  days, and discovered no bimodality in the distribution of rotation periods and no correlation of (I-K) color excess with rotation periods. However, subdividing the sample by mass to select only stars  $> 0.25M_{\odot}$  demonstrated that the higher-mass PMS stars display the bimodal distribution of rotation periods (Herbst et al. 2000). The Stassun et al. (1999) sample is dominated by very low-mass stars which may possess different magnetic star-disk coupling mechanisms. Clarke & Bouvier (2000) argue that the ONC population differs significantly from the Taurus population in that PMS stars in Taurus are generally slow rotators. Hartmann (2002) suggests that this could be because the typical disk-braking time-scale of T Tauri stars is comparable to the ages of T Tauri stars in the ONC. Hence, the mechanism might not have had time to brake most disked stars in the ONC. Stassun et al. (2001) obtained mid-IR data for a sample of stars from the ONC and Tau-Aur selected not to have near-IR excesses. These data indicate no trend of slow rotators with mid-IR excesses in their sample for both clusters. Stassun et al. (2001), like most previous studies, include single, binary and stars that have not been surveyed for companions in the analysis that led to a null result. Interpretation of period and infrared fluxes of binary stars is not straightforward as discussed in the previous subsection. In fact,

for the single stars in their sample (also included in our sample) their results are entirely consistent with ours.

Some of our results echo the observations made by Stassun et al. (2001) that there is no strict dichotomy of disked slow rotators and disk-less fast rotators. A handful of stars qualify as abnormal cases. GK Tau is a fast rotator with a period of 4.65 days. Yet it displays a strong infrared excess,  $E(K_s - N) = 3.20$ . The well-known PMS star SU Aur appears to be a disked ( $E(K_s - N) = 3.33$ ) fast rotator ( $P = 3.50$ d) and IP Tau is definitely a disked ( $(K_s - N) = 2.30$ ) fast rotator ( $P = 3.25$ d). LkCa 21 is a disk-less slow rotator and V819 Tau is disk-less “moderate-to-fast” rotator, classified as a “transition object” by Skrutskie et al. (1990). We queried 2MASS H and  $K_s$ -band magnitudes and derived the  $E(H - K_s)_o$  index for these 5 objects. 4/5 objects have near-IR properties similar to their mid-IR  $E(K_s - N)_o$  properties. GK Tau, SU Aur and IP Tau have significant  $E(H - K_s)_o$  excesses while LkCa 21 has no  $E(H - K_s)_o$  excesses. Perhaps LkCa 21 has very recently lost its disk and has not yet had time to spin up (cf. DI Tau; Meyer et al. (1997b)). Of these “special case” objects, only V819 Tau is included in the study by Edwards et al. (1993). It has no near-IR excess, a marginal (K-N) excess, and a period of 5.6 days. Including all these objects in our analysis, we see a dispersion in the  $E(K_s - N)_o$  vs. rotation period plot comparable to that seen in the  $E(H - K)_o$  analysis of Edwards et al. (1993). It would be interesting to further investigate the physical properties ( $M_*$ ,  $\dot{M}$ ,  $R_*$ , B) of these objects that are expected to determine the co-rotation point in their disks. For example, if  $\dot{M}$  is large enough in the protostellar phase, the inner disk might crush the magnetosphere resulting in a population of rapidly rotating objects (Najita 1995; Covey et al. 2006). Note that the disked fast rotators here have moderate to low accretion rates (Gullbring et al. 1998). A sample of stars with a fixed  $M_*$ ,  $R_*$ , and B should exhibit a correlation between  $P_{rot}$  and  $\dot{M}$  in the x-wind model. Such studies might also elucidate the *dispersion* in the  $(K_s - N)$  vs. period graph.

From a theoretical perspective, we don’t necessarily expect a linear correlation between  $(K_s - N)$  and  $P_{rot}$ . However, our fit demonstrates the low probability that these variables are uncorrelated. Our two-sided K-S test of the periods of disked vs. disk-less stars also hints at a correlation. Rebull et al. (2004) point out that correlations between  $P_{rot}$  and dust-disk or accretion indicators might be difficult to establish given that the spin-up time is of order the age of typical pre-main sequence samples (Hartmann 2002). The fact that we do see a correlation and that our disked and non-disked stars appear to be of similar age (1-3 Myr) suggests that these weak-emission T Tauri stars in Taurus lost their disks very early in their pre-main sequence evolution. Deep far-infrared or millimeter observations might yet reveal whether they retain any disk signatures at all (e.g. Andrews & Williams (2005)). New surveys for disks at all radii enabled with the Spitzer Space Telescope combined with photometric rotation studies will shed considerable light on these remaining questions.

## 5. SUMMARY

1. Analysis of the  $(K_s - N)$  vs. rotation period data for single T Tauri stars in Tau-Aur cloud suggests a correlation implying that disked stars are generally rotating slower than disk-less stars. We selected stars that have been surveyed to be single and have documented photometric rotation periods and available N-band fluxes. There are a few abnormal cases which cause a dispersion in the  $(K_s - N)$  vs. period relation and would be interesting candidates for further study.

2. A histogram of  $(K_s - N)$  colors confirms the result from Skrutskie et al. (1990), Simon & Prato (1995), Kenyon & Hartmann (1995) and Wolk & Walter (1996) that stars between  $1.0m < (K_s - N) < 2.0m$  are rare. The transition from optically thick to optically thin must be much less than the average lifetime of T Tauri stars ( $\ll 1$  Myr).

3. SEDs of a few classical T Tauri stars, including new mid-infrared photometry, confirm that most of these stars are accreting actively from their circumstellar disks. IR excesses are significantly greater than fluxes predicted by the flat-reprocessing disk model of (Hillenbrand et al. 1992). This supports the idea that disks are not flat but are flared and probably have atmospheres (Chiang & Goldreich 1997; D’Alessio et al. 1999; Dullemond et al. 2001).

4. Analyzing Mid-IR fluxes and period data for single stars are best for investigating star-disk rotational interaction because: 1) It is hard to resolve the components of a binary system in the Mid-IR, and 2) photometric period data for binaries are ambiguous. Including binaries can statistically *weaken* any observable correlation caused by star-disk interactions in a population of single stars.

We would like to thank Peter Biezenberger, Christoph Birk, and the staff of UKIRT for their help in commissioning the MAX camera. We would like to thank S. Edwards, S. Wolff and an anonymous referee for helpful comments that improved this manuscript. This material is based on work supported by NASA through the NASA Astrobiology Institute under cooperative agreement CAN-02-OSS-02 issued through the Office of Space Science. This paper makes use of data products from the Two Micron All Sky Survey, which is a joint project of the University of Massachusetts and the Infrared Processing and Analysis Center/California Institute of Technology, funded by the National Aeronautics and Space Administration and the National Science Foundation.

*Facilities:* United Kingdom Infrared Telescope(UKIRT).

## REFERENCES

- Andrews, S.M. & J.P. Williams, 2005, *ApJ*, 631, 1134
- Beckwith, S.V.W. & A. Sargent, 1996, *Nature*, 383, 139
- Beckwith, S.V.W., 1999, *sf99.proc*, 211
- Beichman, C.A, G. Neugebauer, H.J. Habing, P.E. Clegg, T.J. Chester, 1988, *iras*, 1
- Bodenheimer, P., 1995, *ARA&A*, 33, 199
- Bouvier, J., S. Cabrit, M. Fernandez, E.L. Martin & J.M. Matthews, 1993, *A&AS*, 101, 485
- Bouvier, J. 1994, *ASP Conf.*, 64, 151
- Bouvier, J., E. Covino, O. Kovo, E.L. Martin, J.M. Matthews, L. Terranegra & S.C. Beck, 1995, *A&A*, 299, 89
- Bouvier, J., M. Forestini & S. Allain, 1997, *A&A*, 326, 1023
- Camenzind, M., 1990, *RvMA*, 3, 234
- Cameron, A.C. & C.G. Campbell, 1993, *A&A*, 274, 309
- Chiang, E.I. & P. Goldreich, 1997, *ApJ*, 490, 368
- Choi, P.I. & W. Herbst, 1996, *AJ*, 111, 283
- Clarke, C.J. & J. Bouvier, 2000, *MNRAS*, 319, 457
- Cohen, M. 1974, *MNRAS*, 169, 257
- Cohen, M. 1980, *MNRAS*, 191, 499
- Cohen, J.G., J.A. Frogel, S.E. Persson & J.H. Elias, 1982, *ApJ*, 249, 481
- Cohen, M. & R.D. Schwartz, 1976, *MNRAS*, 174, 137
- Cohen, M., R.G. Walker, M.J. Barlow & J.R. Deacon, 1992, *AJ*, 104, 1650
- Covey, K.R., T.P. Greene, G.W. Doppmann & C.J. Lada, 2006, *AJ*, 131, 512
- D'Antona, F. & Mazzitelli, I. 1997, *Mem. Soc. Astron. Italiana*, 68, 807
- D'Alessio, P., N. Calvet, L. Hartmann, S. Lizano & J. Canto, 1999, *ApJ*, 527, 893

- Dullemond, C.P., C. Dominik & A. Natta, 2001, *ApJ*, 560, 957
- Edwards, S. et al., 1993, *AJ*, 106, 372
- Gezari, D.Y., P.S. Pitts & M. Schmite, 1999, *yCat.*, 2225, 0
- Ghez et al., 1991, *AJ*, 102, 2066
- Ghez, A., G. Neugebauer & K. Matthews, 1993, *AJ*, 106, 2005
- Ghez, A., J.P. Emerson, J.R. Graham, M. Meixner & C.J. Skinner, 1994, *ApJ*, 434, 707
- Ghosh, P. & F.K. Lamb, 1979a, *ApJ*, 232, 259
- Ghosh, P. & F.K. Lamb, 1979b, *ApJ*, 234, 296
- Gullbring, E., L. Hartmann, C. Briceno & N. Calvet, 1998, *ApJ*, 492, 323
- Haisch, K.E., E.A. Lada & C.J. Lada, 2001, *ApJ*, 553, L153
- Herbst, W., K.L. Rhode, L.A. Hillenbrand & G. Curran, 2000, *AJ*, 119, 261
- Herbst, W. & R. Mundt, 2005, *ApJ*, 633, 967
- Herbst, W., C.A.L. Bailer-Jones, R. Mundt, K. Meisenheinmer & R. Wackermann, 2002, *A&A*, 396, 513
- Hillenbrand, L.A., S.E. Strom, F.J. Vrba & J. Keene, 1992, *ApJ*, 397, 613
- Hillenbrand et al., 1998, *AJ*, 116, 1816
- Hartmann, L. 2002, *ApJ*, 566, 29
- Jensen, E.L., R.D. Mathieu & G.A. Fuller, 1996, *ApJS*, 458, 312
- Jensen, E.L. & R.D. Mathieu, 1997, *AJ*, 114, 301
- Kenyon, S.J. & Hartmann, L. 1995, *ApJ*, 101, 117
- Koresko, C.D., T.M. Herbst & C. Leinert, 1997, *ApJ*, 480, 781
- Königl, A. 1991, *ApJ*, 370, L39
- Krishnamurthi, A., M.H. Pinsonneault, S. Barnes & S. Sofia, 1997, *ApJ*, 480, 303
- Leinert et al., 1993, *A&A*, 278, 129

- Mamajek, E.E., M.R. Meyer, P.M. Hinz, W.F. Hoffmann, M. Cohen & J.L. Hora, 2004, *ApJ*, 612, 496
- Mathieu, R.D., 2004, *IAUS*, 215, 113
- Matt, S. & R.E. Pudritz, 2005, *ApJ*, 632, 135
- McCaughrean, M.J. & C.R. O'Dell, 1996, *AJ*, 111, 1977
- Meyer, M.R. & S.V.W. Beckwith, 1997, *ASP Conf.*, 134, 245
- Meyer, M.R., N. Calvet & L.A. Hillenbrand, 1997a, *AJ*, 114, 288
- Meyer, M.R., S.V.W. Beckwith, T.M. Herbst & M. Robberto, 1997b, *ApJ*, 489, L173
- Muzerolle, J., N. Calvet & L. Hartman 2001, *ApJ*, 550, 944
- Muzerolle, J., N. Calvet, L. Hartmann & P. D'Alessio, 2003, *ApJ*, 597, L149
- Najita, J., 1995, *RMxAC*, 1, 293
- O'Dell, C.R., 1993, *Science*, 259, 33
- Osterloh, M., E. Thommes & U. Kania, 1996, *A&AS*, 120, 267
- Rebull, L.M., S.C. Wolff & S.E. Strom, 2004, *AJ*, 127,1029
- Robberto, M. & T. Herbst, *Proc. SPIE*, 3354, 711
- Rydgren, A.E., 1984, *PUSNO*, 25, 1
- Shu, F., J. Najita, E. Ostriker, F. Wilkin, S. Ruden & S. Lizano, 1994, *ApJ*, 429, 781
- Ostriker, E.C. & F.H. Shu, 1995, *ApJ*, 477, 813
- Simon, M. & Prato, L., 1995, *ApJ*, 450, 824
- Simon et al., 1995, *ApJS*, 443, 625
- Skrutskie, M.F., D. Dutkevitch, S.E. Strom, S. Edwards, K.M. Strom & M.A. Shure, 1990, *AJ*, 99, 1187
- Skrutskie, M.F., M.R. Meyer, D. Whalen & C. Hamilton, 1996, *AJ*, 112, 2168
- Stassun, K.G., R.D. Mathieu, T. Mazeh & F.J. Vrba, 1999, *AJ*, 117, 2941
- Stassun, K.G., R.D. Mathieu, F.J. Vrba, T. Mazeh & A. Henden, 2001, *AJ*, 121, 1003

Strom, K.M., S.E. Strom, S. Edwards, S. Cabrit & M.F. Skrutskie, 1989, AJ, 97, 1451

von Rekowski, B. & A. Brandenburg, 2004, A&A, 420, 17

Wolk, S.J. & F.M. Walter, 1996, AJ, 111, 2066



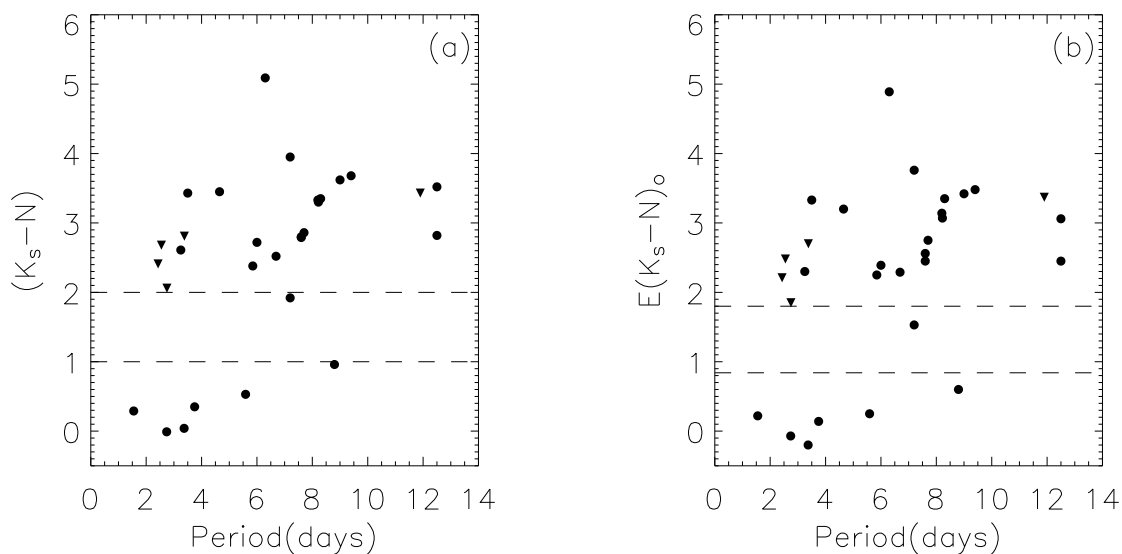


Fig. 1.— Figures 1a and 1b are graphs of  $(K_s - N)$  vs. period and  $E(K_s - N)_o$  vs. period, of a sample of stars from Tau-Aur that are thought to be single. The lower limit for an optically thick circumstellar disk  $(K_s - N) = 2.0m$  (Hillenbrand et al. 1992) and the upper limit for photospheric emission plus extinction  $(K_s - N) = 1.0m$  are indicated by the dashed lines on Figure 1a. The extinction corrected lower limit for an optically thick disk is marked by the dashed line at  $E(K_s - N)_o = 1.8m$  on Figure 1b. Also on Figure 1b, the dashed line at  $E(K_s - N) = 0.84m$  marks the typical value of a  $3\text{-}\sigma$  excess (lower limit for the detection of a disk) for the stars in our sample (Mamajek et al. 2004). The downward pointing triangles represent upper limits in  $(K_s - N)$  and  $E(K_s - N)_o$  above the dispersion in intrinsic color.

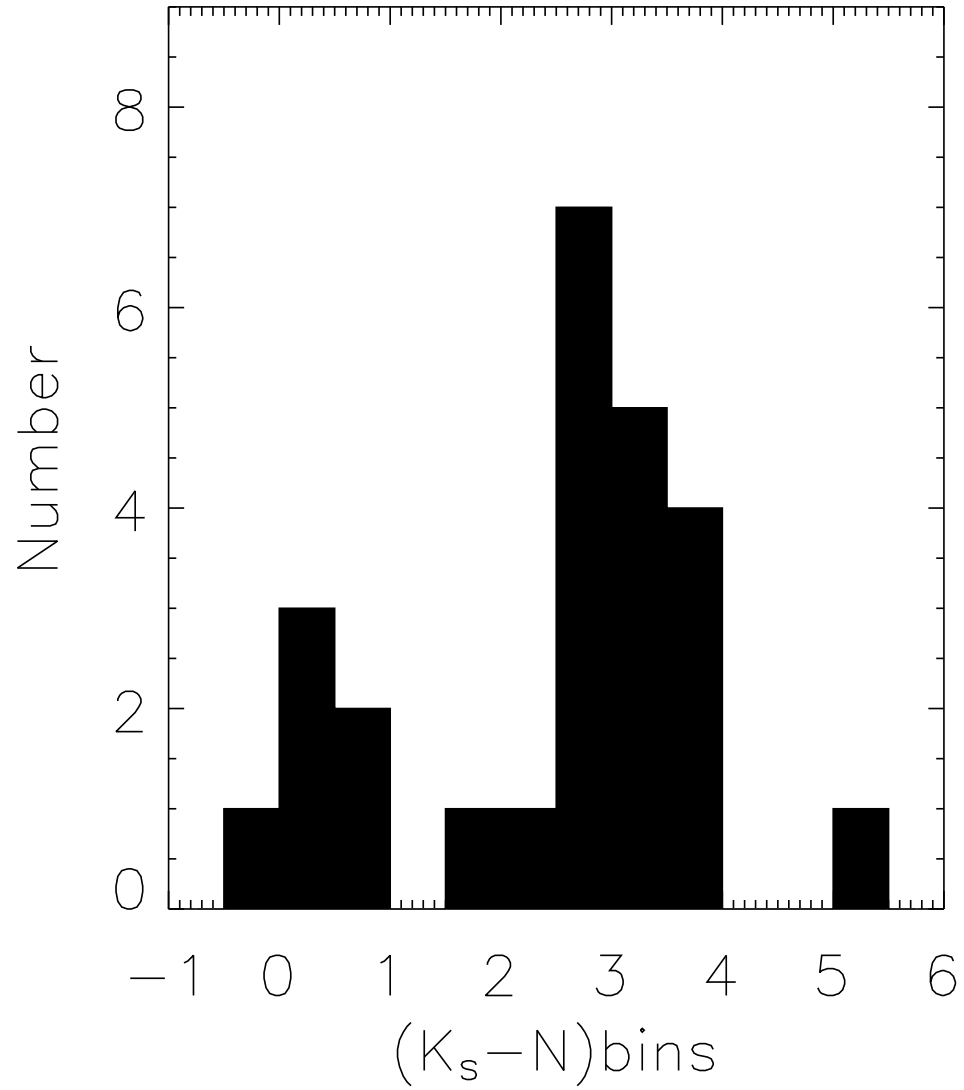


Fig. 2.— Histogram of  $(K_s - N)$  bins (binsize=0.5m) for objects in Figure 1a(excluding upper-limits). Notice the paucity of stars between  $1.0m < (K_s - N) < 2.0m$ .

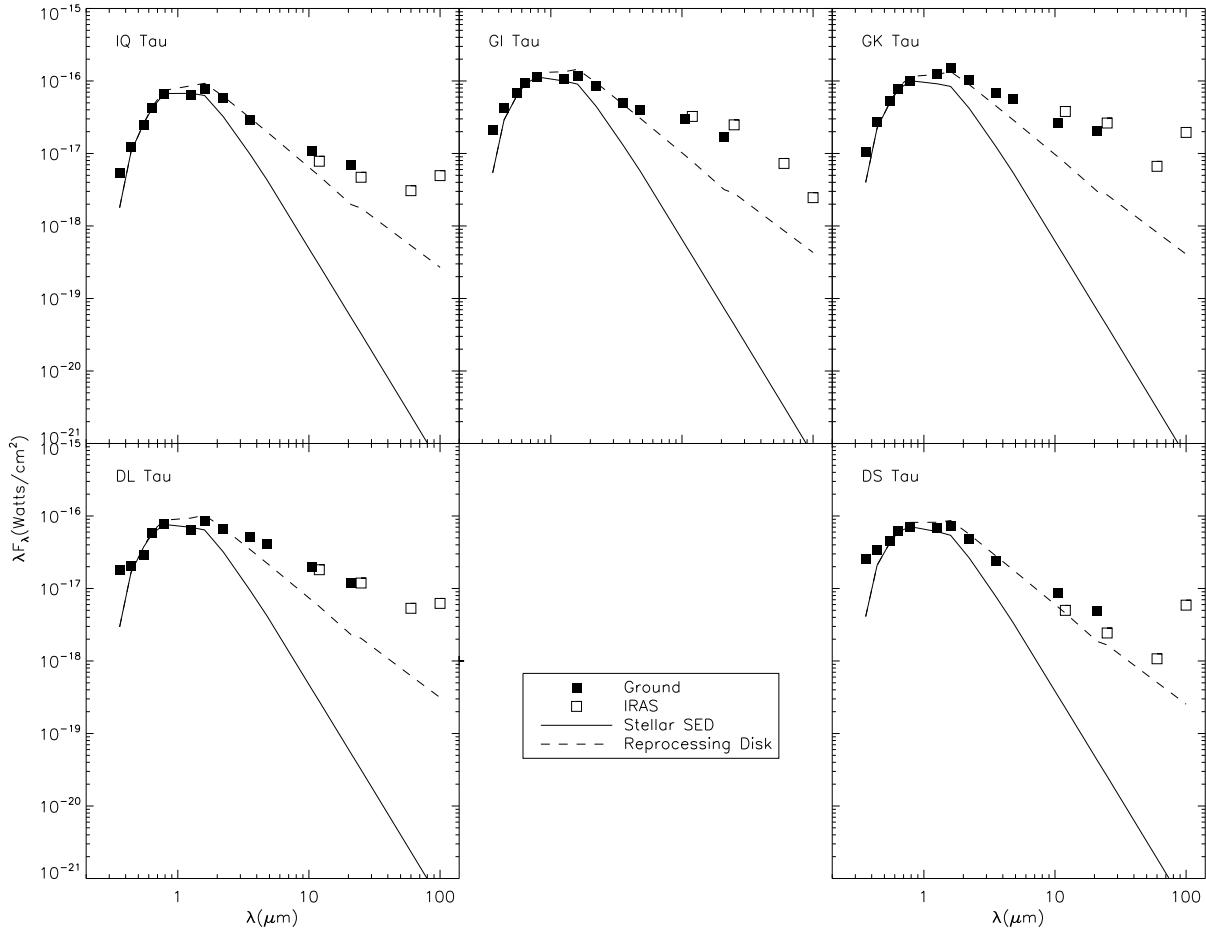


Fig. 3.— These are SEDs of five objects with new M and Q-band observations. The observed fluxes are compared to a model stellar photosphere and an optically-thick, geometrically-thin disk model (Hillenbrand et al. 1992).

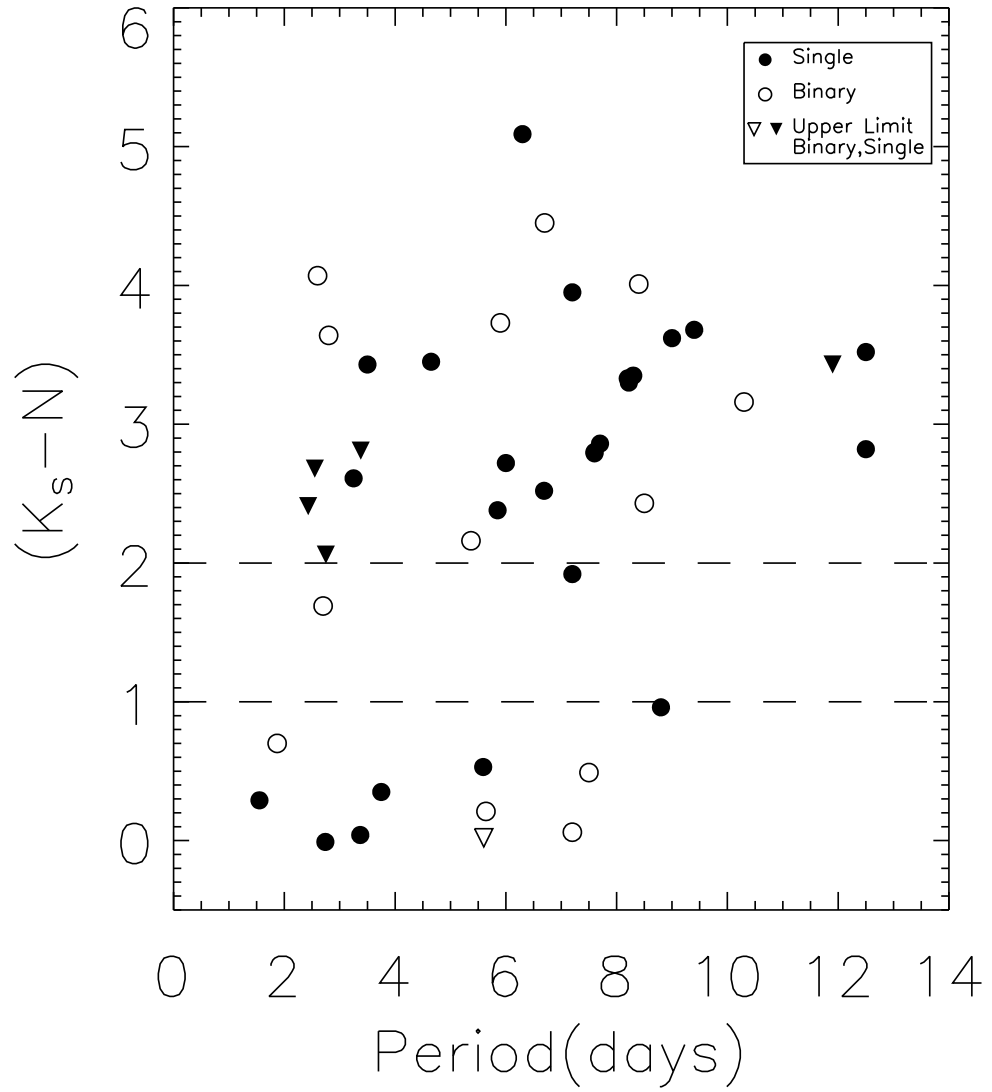


Fig. 4.— This is a  $(K_s - N)$  vs. period graph of single stars (from Figure 1a) and unresolved binaries with period data.

Table 1. MAX Camera Observations of TAU-AUR objects at UKIRT

UT Date	HBC	Object Name	Band	Exposure(sec)	Flux Standards
1997 Feb 6	41	IQ Tau	N	163.84	HR 1370, $\mu$ UMa, $\alpha$ Lyr
-	-	-	Q	98.24	$\beta$ And, HR 1370, $\mu$ UMa, $\alpha$ Lyr
-	56	GI Tau	M	163.84	$\beta$ And, HR 1370, $\mu$ UMa
-	-	-	N	81.92	HR 1370, $\mu$ UMa, $\alpha$ Lyr
-	-	-	Q	98.24	$\beta$ And, HR 1370, $\mu$ UMa, $\alpha$ Lyr
-	57	GK Tau	M	163.84	$\beta$ And, HR 1370, $\mu$ UMa
-	-	-	N	81.92	HR 1370, $\mu$ UMa, $\alpha$ Lyr
-	-	-	Q	98.24	$\beta$ And, HR 1370, $\mu$ UMa, $\alpha$ Lyr
-	58	DL Tau	N	163.84	HR 1370, $\mu$ UMa, $\alpha$ Lyr
-	-	-	Q	98.24	$\beta$ And, HR 1370, $\mu$ UMa, $\alpha$ Lyr
-	75	DS Tau	N	163.84	HR 1370, $\mu$ UMa, $\alpha$ Lyr
-	-	-	Q	98.24	$\beta$ And, HR 1370, $\mu$ UMa, $\alpha$ Lyr
-	384	FT Tau	N	163.84	HR 1370, $\mu$ UMa, $\alpha$ Lyr
-	397	TAP 41	N	327.68	HR 1370, $\mu$ UMa, $\alpha$ Lyr
-	405	V830 Tau	N	327.68	HR 1370, $\mu$ UMa, $\alpha$ Lyr
-	45	UX Tau A	N	245.76	HR 1370, $\mu$ UMa, $\alpha$ Lyr
1997 Feb 8	376	TAP 26	N	614.40	HR 1370, $\mu$ UMa, $\alpha$ Lyr
-	380	HD 283572	N	245.76	HR 1370, $\mu$ UMa, $\alpha$ Lyr
-	382	LkCa 21	N	614.40	HR 1370, $\mu$ UMa, $\alpha$ Lyr
-	392	TAP 40	N	614.40	HR 1370, $\mu$ UMa, $\alpha$ Lyr

Table 2. Data for single T Tauri stars

HBC	Object	Sp. Type	TTs	SED	P(days)	$T_{eff}$ (°K)	$L_*/L_\odot$	log(years)	$M_*/M_\odot$	$K_s$	N	N-ref
41	IQ Tau	M0.5	W	II	12.5 <sup>c</sup>	3785	0.65	5.81	0.38	$7.78 \pm 0.02$	$4.96 \pm 0.06$	This work
56	GI Tau	K6	C	II	7.20 <sup>b</sup>	4205	0.85	6.00	0.58	$7.89 \pm 0.02$	$3.94 \pm 0.04$	This work
57	GK Tau	K7	C	II	4.65 <sup>b</sup>	4060	1.17	5.67	0.45	$7.47 \pm 0.02$	$4.02 \pm 0.04$	This work
58	DL Tau	K7	C	II	9.40 <sup>a</sup>	4060	...	...	...	$7.96 \pm 0.02$	$4.28 \pm 0.03$	This work
75	DS Tau	K5	C	II	7.70 <sup>c</sup>	4350	0.65	6.38	0.75	$8.04 \pm 0.03$	$5.18 \pm 0.09$	This work
37	TAP 26	K7	W	III	2.55 <sup>b</sup>	4060	0.41	6.45	0.64	$9.27 \pm 0.02$	$>6.59$	This work
380	HD 283572	G5	W	III	1.55 <sup>b</sup>	5770	6.50	6.70	1.85	$6.87 \pm 0.02$	$6.58 \pm 0.18$	This work
382	LkCa 21	M3	W	III	8.80 <sup>a</sup>	3470	0.62	5.27	0.24	$8.45 \pm 0.02$	$7.49 \pm 0.25$	This work
384	FT Tau	C	...	II	8.30 <sup>c</sup>	...	...	...	...	$8.60 \pm 0.02$	$5.25 \pm 0.07$	This work
392	TAP 40	K5	W	III	3.38 <sup>b</sup>	4350	0.32	7.03	0.87	$9.50 \pm 0.02$	$>6.69$	This work
397	TAP 41	K7	W	III	2.43 <sup>b</sup>	4060	0.50	6.28	0.59	$8.85 \pm 0.02$	$>6.44$	This work
405	V830 Tau	K7	W	III	2.75 <sup>b</sup>	4060	0.68	6.02	0.52	$8.42 \pm 0.02$	$>6.36$	This work
25	CW Tau	K3	C	II	8.20 <sup>b</sup>	4730	1.35	6.27	0.97	$7.13 \pm 0.02$	$3.80 \pm 0.15$	C74
32	BP Tau	K7	C	II	7.60 <sup>b</sup>	4060	0.95	5.79	0.47	$7.74 \pm 0.02$	$4.95 \pm 0.11$	CS76
33	DE Tau	M2	C	II	7.60 <sup>b</sup>	3580	0.81	5.23	0.26	$7.80 \pm 0.02$	$5.00 \pm 0.25$	C74
37	DG Tau	K7-M0	C	II	6.30 <sup>b</sup>	3950	...	...	...	$6.99 \pm 0.02$	$1.90 \pm 0.05$	C74
38	DH Tau	M1	C	II	7.20 <sup>b</sup>	3720	0.68	5.75	0.34	$8.18 \pm 0.03$	$6.26 \pm 0.04$	M97b
63	AA Tau	K7	C	II	8.22 <sup>b</sup>	4060	0.74	5.96	0.51	$8.05 \pm 0.02$	$4.75 \pm 0.25$	C74
65	DN Tau	M0	C	II	6.00 <sup>b</sup>	3850	0.91	5.66	0.37	$8.02 \pm 0.02$	$5.30 \pm 0.30$	C74
67	DO Tau	M0	C	II	12.5 <sup>c</sup>	3850	1.20	5.50	0.34	$7.30 \pm 0.02$	$3.78 \pm 0.05$	C74
74	DR Tau	K7	C	II	9.00 <sup>b</sup>	4060	...	...	...	$6.87 \pm 0.02$	$3.25 \pm 0.15$	C74
77	GM Aur	K3	C	II	11.9 <sup>b</sup>	4730	0.83	6.63	1.03	$8.28 \pm 0.02$	$>4.85$	C74
79	SU Aur	G2	W	II	3.50 <sup>a</sup>	5860	10.7	6.42	2.31	$5.99 \pm 0.02$	$2.56 \pm 0.05$	C80
370	LkCa 4	K7	W	III	3.37 <sup>b</sup>	4060	0.85	5.86	0.49	$8.32 \pm 0.02$	$8.28 \pm 0.27$	S90
378	V819 Tau	K7	W	III	5.59 <sup>b</sup>	4060	0.81	5.89	0.50	$8.42 \pm 0.02$	$7.89 \pm 0.16$	S90
385	IP Tau	M0	W	II	3.25 <sup>b</sup>	3850	0.43	6.17	0.48	$8.35 \pm 0.02$	$5.74 \pm 0.06$	S90
388	TAP 35	K1	W	III	2.74 <sup>b</sup>	5080	1.40	6.73	1.37	$8.30 \pm 0.02$	$8.31 \pm 0.22$	S90
399	V827 Tau	K7	W	III	3.75 <sup>b</sup>	4060	0.89	5.83	0.48	$8.23 \pm 0.02$	$7.88 \pm 0.16$	S90
419	LkCa 15	K5	W	II	5.85 <sup>b</sup>	4350	0.74	6.27	0.72	$8.16 \pm 0.02$	$5.78 \pm 0.11$	S90
429	V836 Tau	K7	W	III	6.69 <sup>b</sup>	4060	0.47	6.33	0.60	$8.60 \pm 0.02$	$6.08 \pm 0.09$	S90

<sup>a</sup>Bouvier et al. (1993)

<sup>b</sup>Bouvier et al. (1995)

<sup>c</sup>Osterloh et al. (1996)

Note. — Spectral Type, SED class,  $T_{eff}$  and  $L_*$  are from Kenyon & Hartmann (1995). TTS type was taken from Strom et al. (1989). log(years) and  $M_*$  derived from tracks of D’Antona & Mazzitelli (1997). N-Ref. C74 - Cohen (1974), C80 - Cohen (1980), M97b - Meyer et al. (1997b) and S90 - Skrutskie et al. (1990).  $3\sigma$  upper-limits are quoted for non-detections.

Table 3. Photometric Data for SEDs.

Object	U	B	V	R	I	J	H	K <sub>s</sub>	L	M	N	12 $\mu$ m	Q	25 $\mu$ m	60 $\mu$ m	100 $\mu$ m
GI Tau	15.28	14.79	13.21	12.15	11.06	9.42	8.46	7.89	6.83	6.11 $\pm$ 0.21	3.94 $\pm$ 0.04	3.43	2.28 $\pm$ 0.09	1.30	-0.22	-0.70
GK Tau	14.56	14.01	12.54	11.58	10.62	9.02	8.02	7.47	6.46	5.72 $\pm$ 0.15	4.02 $\pm$ 0.04	3.22	2.07 $\pm$ 0.10	1.23	-0.12	-2.95
DL Tau	13.91	14.26	13.12	11.85	10.89	9.73	8.63	7.96	6.76	6.04	4.28 $\pm$ 0.03	4.02	2.66 $\pm$ 0.12	2.09	0.12	-1.71
IQ Tau	15.43	14.99	13.45	12.28	11.11	9.74	8.74	7.78	7.39	...	4.96 $\pm$ 0.06	4.94	3.25 $\pm$ 0.21	3.10	0.72	-1.46
DS Tau	13.11	13.35	12.37	11.56	10.80	9.59	8.75	8.04	7.57	...	5.18 $\pm$ 0.09	5.41	3.61 $\pm$ 0.30	3.81	1.86	-1.65

Note. — Values from this study have uncertainties quoted. UBVRI and JHLM are from KH95. K<sub>s</sub> is from the 2MASS point source catalog. 12 $\mu$ m, 25 $\mu$ m, 60 $\mu$ m and 100 $\mu$ m values are from the IRAS point source catalog (Beichman et al. 1988).

Table 4. Data for Binaries with Periods and N-band magnitudes.

HBC	Object	P(days)	Sep(")	$T_{eff}$ (°K)	$L_*/L_\odot$	$K_s$	N	N-ref.
29	V410 Tau	1.87	0.12 <sup>a</sup>	4730	2.14	7.63	6.93	S90
35	T Tau	2.80	0.71 <sup>a</sup>	5250	8.91	5.33	1.69	G91
36	DF Tau	8.50	0.09 <sup>b</sup>	3470	1.60	6.73	4.30	C74
39	DI Tau	7.50	0.12 <sup>b</sup>	3850	0.62	8.39	7.90	M97b
43	UX Tau A	2.70	2.70 <sup>c</sup>	4900	1.35	7.55	$5.86 \pm 0.10$	This work
45	DK Tau	8.40	2.53 <sup>b</sup>	4060	1.32	7.10	3.09	CS76
50	XZ Tau	2.60	0.31 <sup>a</sup>	3470	0.71	7.29	3.22	CS76
54	GG Tau	10.3	0.29 <sup>a</sup>	4060	1.50	7.36	4.20	C74
66	HP Tau	5.90	0.02 <sup>b</sup>	4730	1.30	7.63	3.90	C74
68	VY Tau	5.37	0.66 <sup>b</sup>	3850	0.47	8.96	6.80	SP95
76	UY Aur	6.70*	0.88 <sup>a</sup>	4060	2.00	7.24	2.79	KHL97
368	LkCa 3	7.20	0.49 <sup>a</sup>	3720	1.66	7.42	7.36	S90
379	LkCa 7	5.64	1.05 <sup>c</sup>	4060	0.89	8.26	8.05	S90
420	IW Tau	5.60	0.27 <sup>b</sup>	4060	0.87	8.28	$> 8.26$	SMVMH01

\*Osterloh et al. (1996). All other periods are from Bouvier et al. (1995)

<sup>a</sup>Ghez et al. (1993)

<sup>b</sup>Simon et al. (1995)

<sup>c</sup>Leinert et al. (1993)

Note. — UX Tau’s companions were unresolved in the N-band. We are unsafely assuming that UX Tau A is the dominant source of N-band flux(See section 4.3).

$T_{eff}$  and  $L_*$  values are from Kenyon & Hartmann (1995).  $K_s$  magnitudes are from the 2MASS point source catalog. C74 - Cohen (1974), CS76 - Cohen & Schwartz (1976), S90 - Skrutskie et al. (1990), G91 - Ghez et al. (1991), SP95 - Simon & Prato (1995), M97b - Meyer et al. (1997b), KHL97 - Koresko, Herbst & Leinert (1997), SMVMH01 - Stassun et al. (2001).  $3\sigma$  magnitude upper-limits are quoted for non-detections.